Supporting Information

Automated Femtoliter Droplet-Based Determination of Oil-Water Partition Coefficient

Miaosi Li,[†*] Brendan Dyett,[‡] and Xuehua Zhang [§*]

[†] *School of Engineering, RMIT University, Melbourne, VIC, 3000, Australia.*

[‡] *School of Science, RMIT University, Melbourne, VIC, 3000, Australia.*

[§] *Department of Chemical and Materials Engineering, University of Alberta, Edmonton, Alberta T6G 1H9, Canada.*

*E-mail: miaosi.li@rmit.edu.au, xuehua.zhang@ualberta.ca

Methods

Materials

The droplet liquid, 1-octanol (99%), the analytes for the detection of partition coefficient, including rhodamine 6G, fluorescein (FR), triclosan, carbamazepine, caffeine, gallic acid and methylene blue (MB), and the salts for preparing the buffer solution were all purchased from Sigma-Aldrich. Ethanol (99%) was purchased from ChemSupply, Pty. Ltd, Australia, and water was obtained from a Milli-Q purification unit (Millipore Corporation, Boston, MA). Silicon wafers were purchased from Mitsubishi Silicon (USA). Octadecyltrimethylchlorosilane (OTS, 98%) purchased from Sigma-Aldrich was used for the hydrophobilization of the wafers. The OTS-coated substrates were prepared by following the protocol reported in previous work.[1] After coating, the static contact angle of OCT on the OTS-Silicon substrate in water was measured by the equipment and software from Dataphysics (Germany), which is 42 ± 3º.

Process of the partition/distribution coefficient detection

The partition/distribution coefficient of the analyte was determined by the continues solvent exchange performed in a hand-made flow chamber with the programmable syringe pumps (New Era Pump System). The width (w) and height (h) of the chamber were fixed at 15 mm and 0.75 mm in this work. The sequence of the liquid injecting into the flow chamber, the solution content and the flow conditions for completing one detection cycle are summarised in Table S1. The average mean flow velocity, U, was determined by the equation of $Q = hwU$.[2]

Table S1. Solvent exchange sequence and conditions for the detection of partition/distribution coefficient.

Seq.	Solution content	Flow rate (Q, μL/min)	Velocity (U, mm/s)	Volume (mL)	Performance
1	5% (v/v) OCT in 50% ethanol/water solution	5000	80	2	Droplet liquid introduction
2	Water (OCT saturated)	400	6.4	5	Droplet formation
3	Target compound in aqueous solution	200-2000	3.2-32	3	Liquid-liquid extraction
4	Ethanol	5000	80	10	Droplet removal & surface clean

For the detection of partition coefficient, the target analyte was dissolved in the pure water solution at a certain concentration. For the detection of distribution coefficient, the analyte was dissolved in the solution of different pHs prepared by acetic acid/sodium acetate buffer and phosphate-buffered saline (PBS). The Nikon upright fluorescence microscope was used to capture the optical and fluorescence images of the droplets. All the detections were under the room temperature of 20±2 ºC.

Quantification of the concentration in the droplets by microspectrophotometer

The UV-vis microspectrophotometer (CRAIC Technologies ™) [3] was employed to obtain the spectrum of the analytes in the droplets and in the surrounding water phase. In this work we acquired the signal through the light reflected from the specimen on the surface of the silicon wafer. Figure S1a copied from the equipment website [3] shows the sketch of how the microspectrophotometer operates. Figure S1b shows the real-time image obtained on the software of the microspectrophotometer. The black square, as labelled by the red dotted area, is the adjustable aperture whose size can be chose from 50×50 to 2×2 μm. During detection, we moved the black square to the top of a single droplet and to the blank area surrounding the droplet, to achieve the spectrum of the compound in droplet and in water phase, respectively. The UV-vis absorbance (A) of the compound determined by the microspectrophotometer follows the Beer-Lambert law, in which:

$$A \propto L \tag{S1}$$

where L is the effective path length of the scanned media. Therefore when we acquire the signal from the droplet, the effective scanned area of a droplet is illustrated in Figure S1c. The effective path length is defined by:

$$L = \frac{dV}{a^2} \tag{S2}$$

with

$$dV = z(x, y)dxdy \tag{S3}$$

where a is the dimension of the scanned area and dV is the effectively scanned volume of the droplet.

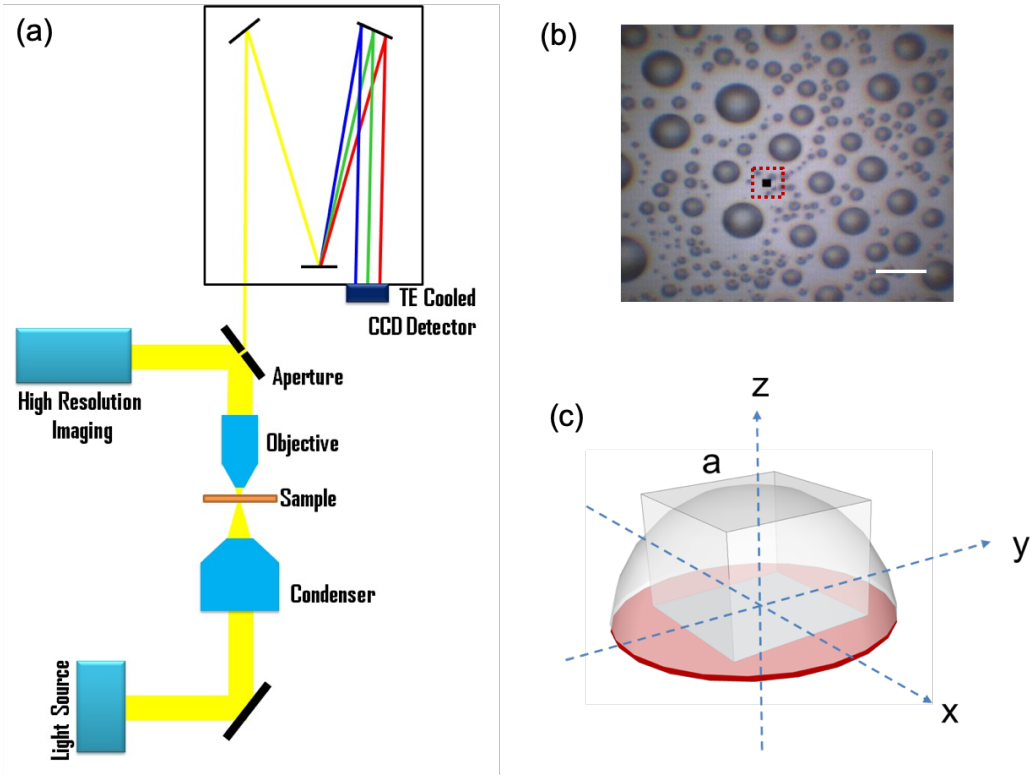

Figure S1. (a) Sketch of the equipment set-up of the microspectrophotometer. (b) The detection image from the microspectrophotometer on the surface droplets. Scale bar: 60 μm. (c) Sketch showing the effectively scanned area of the droplet.

To find out the possible detection error induced by the aperture size, droplet diameter and droplet curvature, in the preliminary study we tested the absorbance of a colour dye in the droplets. First of all, the absorbance on the droplet of different sizes with the fixed size of the aperture was obtained, as plotted in Figure S2a. The absorbance is linearly fitted with the diameter of the droplets, indicating the detection follows the Beer-Lambert's law. With known concentration of the dye and the height of the droplets, the molar extinction coefficient of the compound can be calculated, which is in agreement with the one obtained by the regular UV-vis spectrometer, demonstrating the reliability of this microscope-equipment spectrophotometer.

Furthermore, we detected the absorbance obtained on fixed droplets but with different aperture sizes, as results shown in Figure S2b. From eq. S2 we find out for a flat specimen with constant height, the size of the aperture should not influence the absorbance. However, Figure S2b shows that the absorbance decreases with the increase of the aperture size. Clearly this detection error is due to the curved surface of the droplets. As illustrated in Figure S2c, the integrated height in the scanning area (red coloured area) will be lower than the actual height of the droplets, due to the volume loss from the curved surface of the droplet. The larger the

red area is, the smaller the effective path length will be. Accordingly, the absorbance will decrease. However, when the aperture size (a) is much smaller than the droplet diameter (D), the influence of the curvature of the droplet can be reduced, as demonstrated in Figure S2d. The results in Figure S2b also suggest that the difference of absorbance obtained by the aperture size of 5 and 10 µm is quite small, indicating the influence of the curvature can be neglected for these small aperture sizes. Therefore during this work we chose the droplet diameter from 30-50 µm, and the scan area diameter of 5 µm for the quantification. As such $dV \sim H_d a^2$, and $L = H_d$, where H_d is the height of the droplet. With this assumption the effective pathlength L in the octanol phase is the height of the droplet. When we acquire the signal from the surrounding area of the droplets, the effective pathlength is the height of the water phase, which is determined by the height of the flow channel. Consequently, with known pathlength and absorbance, the partition coefficient can finally be calculated by eq. 1-5 in the manuscript.

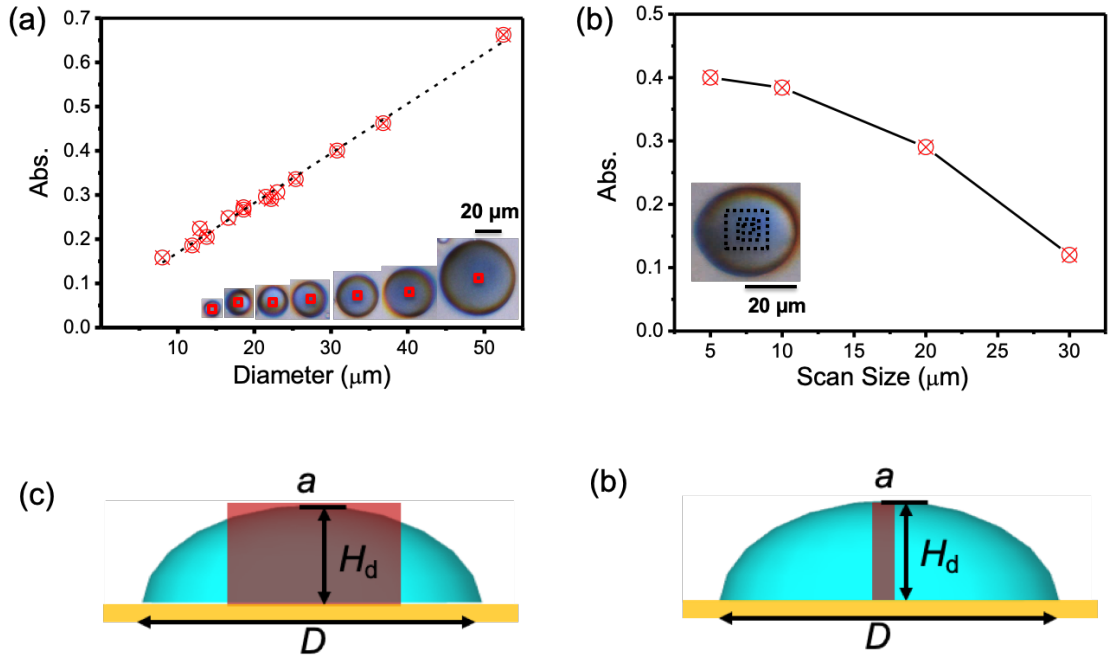

Figure S2. (a) Plots of the intensity of the absorbance on different size of droplets with fixed size of the aperture of the microscope. (b) Plots of the intensity of the absorbance on a fixed droplet with different size of the aperture of the microscope. (c-d) Sketch of defining the effective pathlength of different aperture size (a) within the droplets.

Detection of R6G partition coefficient

The intensity of the absorbance obtained on the droplets of different sizes in contacting with R6G solution was plotted as function of the droplet height in Figure S3a. The intensity normalised by droplet height is then plotted in Figure S3b as function of the droplet diameter. The identical normalised intensity indicates the accuracy of this droplet-based method regardless of droplet size deviation.

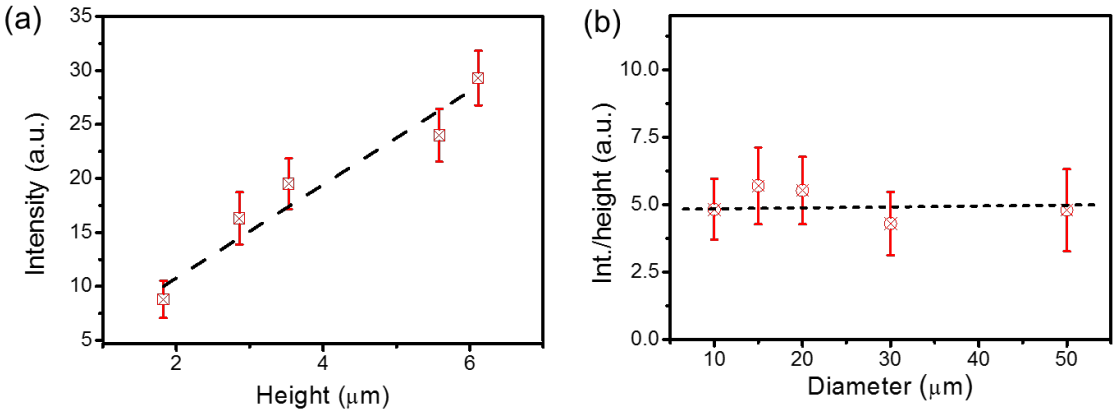

Figure S3. (a) Plot of the absolute intensity of the absorbance of R6G obtained on the droplets against the droplet height determined by Eq(5). (b) Plot of the normalised intensity by the droplet height against the droplet diameter.

The influence on the detection of partition coefficient

The influence of the ethanol content in the original solution containing droplet liquid has been studied and the results are summarised in Table S2.

Table S2. The influence of the ethanol content on the partition coefficient of R6G.

OCT:Ethanol (v/v)	Ethanol Content (v/v)	log$K_{o\text{-}w}$, droplet	log$K_{o\text{-}w}$, literature, ethanol absence
1:50	49.5%	ND *	2.69 [4]
1:25	49.0%	2.51	
1:16.7	48.5%	2.67	
1:12.5	48.1%	2.75	
1:10	47.6%	2.71	

*ND: not detectable, due to the size of the droplets is out of the detectable range.

The influence of the salts on the formation of the droplets has been studied. After the droplets are formed on the surface. Larger quantity of the NaCl aqueous solution (0.1M) was introduced to the flow channel. The results shown in Figure S4 indicated the droplets are stable with the addition of salts in the flow. Although small droplets can be dissolved when there were more than 8 mL of salt solution introducing to the flow channel, our detection will not be influenced by the dissolution, as only ~3 mL of the analyte solution will be injected into the channel (Table S1).

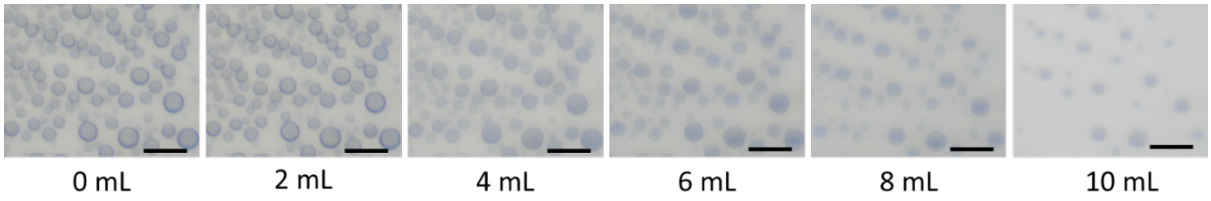

Figure S4. Optical images of the surface octanol droplets with the addition of NaCl solution (0.1mM) of increased volumes. Length of scale bar: 50 μm.

Detection of partition/distribution coefficient by shake-flask method

We determined the distribution coefficient of several compounds by the standard shake-flask method. Specifically, a certain concentration of the substance dissolved in different types of solutions was mixed with same volume of OCT in a separation tunnel. After shaking the liquid mixture for 20-30 seconds, the tunnel was left for more than 24 hours in ambient environment. The water and OCT phase was then separated and the concentration of the substance in these two phases was determined by a UV-vis spectrometer (Shimazu), respectively.

References

(1) Zhang, X.; Lu, Z.; Tan, H.; Bao, L.; He, Y.; Sun, C.; Lohse, D. *Proc. Natl. Acad. Sci.* **2015**, 112 (30), 9253–9257.
(2) Yu, H.; Lu, Z.; Lohse, D.; Zhang, X. *Langmuir* **2015**, 31(46), 12628-12634.
(3) http://www.microspectra.com/support/the-science